

# Measuring voltage in a $\text{YBa}_2\text{Cu}_3\text{O}_8$ superconductor induced by a moving magnet

W. C. Chan, C. B. Lin, H. Chao, and C. H. Chiang

*Physics Department, Tamkang University, Tamsui, Taipei Hsien, Taiwan 25137, Republic of China*

(Received 21 March 2005; revised manuscript received 22 August 2005; published 22 November 2005)

This study examined a pair of permanent magnets rotating above a tape-shaped single grain  $\text{YBa}_2\text{Cu}_3\text{O}_8$  (YBCO) superconducting sample (SS) with and without an applied bias current. The root-mean-square voltages ( $V_{\text{rms}}$ ) induced by the forced movements of the vortices inside the SS were measured. At SS temperatures higher than the critical temperature ( $T_c$ ), the induced  $V_{\text{rms}}$  was a constant, as expected from Faraday's law. However, at a temperature in the superconducting transition region, the induced  $V_{\text{rms}}$  is a sensitive function of both the motion of the magnet and the bias current applied to the SS. At temperatures below the transition region, the induced  $V_{\text{rms}}$  did not drop to zero immediately. Instead, it dropped only to a particular value and then decreased as the temperature decreased. The experimental results obtained at temperatures in the superconducting transition region can be understood by considering the superposition of the two induced voltages. One is induced according to Faraday's law, and the other one is induced by the flux flow inside the SS, which is caused by the bias current. At temperatures below the transition region, an explanation of how the magnetic field of a moving magnet passes through the superconductor is provided, and is consistent qualitatively with the experimental results. In this explanation, some of the magnetic field is assumed first to fill in and then to be pulled out from all sides of the SS in accordance with Bean's model as the moving magnet passes through the SS from above.

DOI: [10.1103/PhysRevB.72.172510](https://doi.org/10.1103/PhysRevB.72.172510)

PACS number(s): 74.25.Op, 74.25.Qt, 74.72.Bk

## I. INTRODUCTION

It is well known that when both magnetic field  $\mathbf{B}$  and current density  $\mathbf{J}$  are applied to a type II superconductor, the vortex lattice sometimes can break free from the pinning force and move in the direction of the Lorentz force density  $\mathbf{f}=\mathbf{J}\times\mathbf{B}$ . This vortex lattice flow was first discovered by Kim *et al.*,<sup>1</sup> who measured the voltage drop across a current-carrying superconducting slab in the mixed state. If the vortices are moving with a mean velocity  $\mathbf{v}$ , an electric field  $\mathbf{E}=-\mathbf{v}\times\mathbf{B}$  appears. The measurement of this induced electric field  $\mathbf{E}$  as a function of temperature  $T$  has become a common method used to investigate the motion of a vortex lattice inside a superconductor. It has been used extensively for studying the Hall effect<sup>2-7</sup> and vortex lattice phase transition.<sup>8-20</sup> In this Brief Report, the same method is used to investigate the motion of the vortices. However, the motion of the vortices was caused mainly by a moving permanent magnet (PM), rather than the Lorentz force associated with the flow of a transport current in the superconductor. This study addresses how the magnetic field of a moving PM passes through a type II superconductor.

## II. EXPERIMENTAL SETUP

Figure 1(a) shows the wiring of our equipment. Signals from the SS inside the cold chamber of the closed-cycle helium gas cryogenic system were sent to the input of the lock-in amplifier. The rotational frequency of a pair of Nd-Fe-B permanent magnets of dimensions  $11.9\times 10.1\times 4.8\text{ mm}^3$  was monitored using a photodiode detector with a red laser beam. The output of the photodiode detector, after it had been amplified, was displayed on oscilloscope A and also used as the external lock-in signal for the lock-in amplifier. The instant output of the lock-in amplifier was displayed

on oscilloscope B. Figure 1(b) shows in more detail the arrangement of the SS inside the cold chamber. The four-point-of-contact method was used, as it was for making the resistance-temperature measurements. Two are used to apply the bias current  $I_b$  and two are used to measure the induced voltage inside the SS. The rotational frequency of the PM was controlled by a small dc motor. At temperatures under 100 K, the resistant torque on the dc motor due to the flow of induced current inside the base of the SS becomes very large. Hence, the base was specially shaped as shown in Fig. 1(b) and aluminum was used instead of copper. The  $\text{YBa}_2\text{Cu}_3\text{O}_8$  (YBCO) SS was prepared by the seeded-melt growth method<sup>21</sup> and cut into a rectangular shape of dimensions  $8.9\times 3.8\times 1.4\text{ mm}^3$  with the  $c$  axis parallel to its shortest side.

## III. EXPERIMENTAL RESULTS AND DISCUSSION

The shortest distance between the moving magnets and the SS was set to 1 mm, where the magnetic field ( $B_z$ ) was about 3.5 kG. The rotational frequency ( $f$ ) of the PM was set to 25 Hz. Figure 1(b) shows the direction of rotation. The maximum output of our current source (Keithley model 220), around 100 mA, is used to maximize the effect of the bias current on our measurements. Therefore, in all our measurements, the bias current  $I_b$  was set to 0 and  $\pm 100$  mA. Figure 1(b) also shows the sign of the bias current. Measuring the resistance against temperature of the SS with a current of 100 mA at a magnetic field of 3.5 kG yields a temperature in the middle of the transition region of around 90 K. The width of the transition region is around 6 K. The lock-in amplifier can give out two kinds of readings. One is called the root-mean-square reading and is obtained by setting the time constant of the lock-in amplifier to a large value. In all our measurements with the root-mean-square readings, the

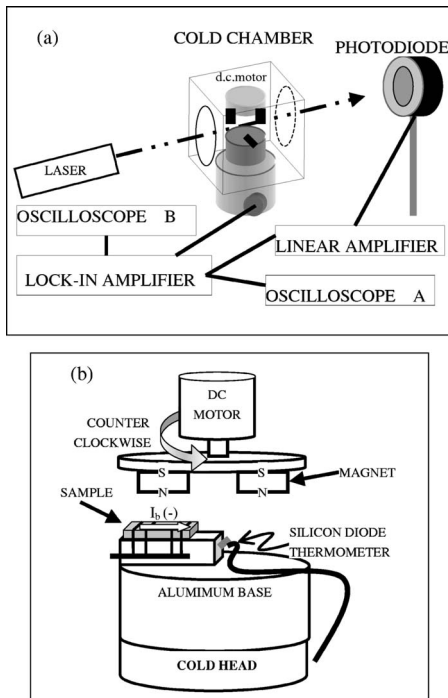


FIG. 1. Experimental setup. (a) Wiring of the lock-in amplifier. (b) Arrangement of the SS inside the cold chamber of the closed-cycle helium gas cryogenic system.

time constant was set to 1 s, which is much larger than  $(1/f)$  s. The other is called the instant reading, and is obtained by setting the time constant of the lock-in amplifier to a small value and the readings must be displayed on an oscilloscope. In measuring all of the instant readings, the time constant was set to  $300 \mu\text{s}$ , which is much smaller than  $(1/f)$  s.

Figure 2 shows the root-mean-square-induced voltage ( $V_{\text{rms}}$ ) as a function of temperature ( $T$ ) inside the SS with different bias current  $I_b$  and different directions of rotation of the PM. The curves can be divided into three different regions: the high-temperature region ( $T > 93$  K), the transition temperature region ( $87 < T < 93$  K), and the low-temperature region ( $T < 87$  K). In the high-temperature region,  $V_{\text{rms}}$  is almost a constant with respect to both temperature  $T$  and bias current  $I_b$ , as expected from Faraday's law. However, in the transition temperature region,  $V_{\text{rms}}$  strongly depends on both the direction of rotation of the PM and the bias current  $I_b$ .

Figure 3 shows the images of the display of the instant voltage  $V_i$  on oscilloscope B in the middle of the transition temperature region (91 K) with different bias current  $I_b$  and different directions of rotation of the PM. Each picture shows two signals, one for the pass of each magnet over the SS. The schematic diagram in Fig. 4 is drawn to explain Fig. 3. Figure 4(a) shows the two magnets together with their magnetic-field lines for five different positions of the superconductor-normal conductor (S-N) loop. Figure 4(b) shows approximately the perpendicular component of the magnetic field ( $B_{\perp}$ ) to the surface of the S-N loop as a function of position. From Fig. 1(b), when viewed in the same direction as the bias current  $I_b(-)$ , the surface of the S-N loop is not horizontal. Therefore, Fig. 4(b) is not symmetric about the

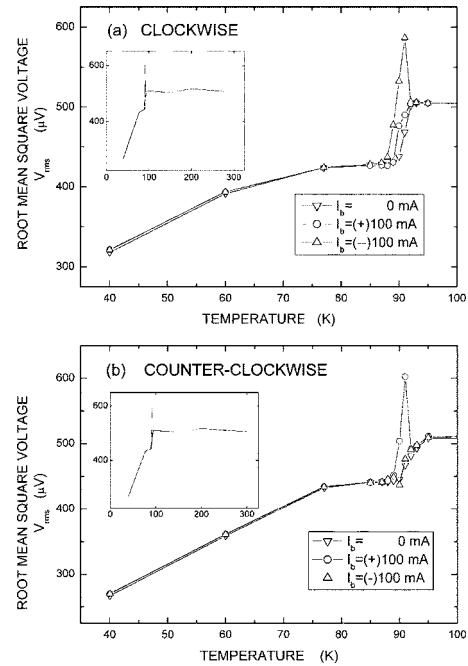


FIG. 2. Root-mean-square-induced voltage ( $V_{\text{rms}}$ ) inside the SS due to the clockwise (a) and counterclockwise (b) rotation of the PM's with different bias current  $I_b$ . The insets show the full range of temperature in our measurements.

center of the magnet. Figure 4(c) shows the induced voltage ( $V_{\text{ilc}}$ ) inside the S-N loop as it moves from left to right relative to the magnets for clockwise rotation. The sign of  $V_{\text{ilc}}$  depends upon how the two terminals of the S-N loop are connected to the oscilloscope. It is chosen such that Fig. 4(c)

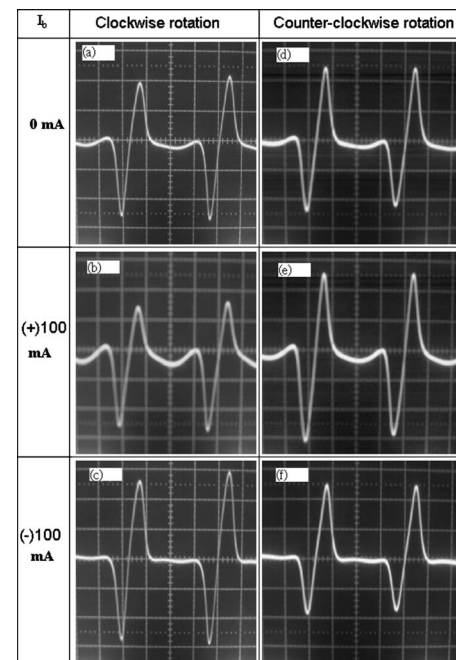


FIG. 3. Instant induced voltage  $V_i$  inside the SS at  $T=91$  K caused by the clockwise and counterclockwise rotation of the PM with different bias current  $I_b$ . The vertical scale is  $0.25 \text{ mV/div}$  and the horizontal scale is  $5 \text{ ms/div}$ .

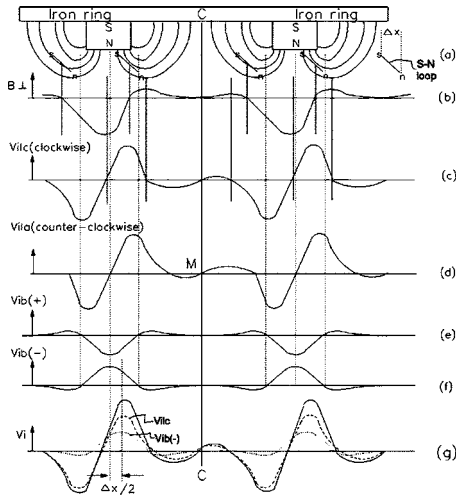


FIG. 4. Schematic diagram showing how to obtain the induced voltage  $V_i$  as shown in Fig. 3. (a) Two magnets with some magnetic-field lines and five different positions of the S–N loop. (b) Perpendicular component of the magnetic field to the surface of the S–N loop as a function of position. (c) and (d) Induced voltages  $V_{il}$  inside the S–N loop for clockwise and counterclockwise rotation of the magnets, respectively. (e) and (f) Voltage  $V_{ib}$  induced by flux flow inside the SS caused by positive and negative bias currents, respectively. (g) Induced voltage  $V_i$  inside the S–N loop for clockwise rotation with negative bias current.

looks similar to Fig. 3(a), which displays the induced voltage without bias current. Figure 4(d) shows the induced voltage ( $V_{ila}$ ) inside the S–N loop as the loop moves from right to left relative to the magnets for counterclockwise rotation of the magnets. The curve can be obtained by flipping the curve in Fig. 4(c) twice, once horizontally and once vertically with the zero point  $M$  fixed at the vertical central line,  $CC$ , as shown in the figure. It would be the same as Fig. 4(c) if the surface of the S–N loop were lying horizontally. Again, Fig. 4(d) is quite similar to Fig. 3(d).

Induced voltages with bias currents can be understood by the use of the principle of superposition. A bias current does not affect the normal side of the S–N loop, but it induces a voltage ( $V_{ib}$ ) on the superconducting side<sup>22–24</sup> with  $V_{ib} = (B_z/B_{c2})(R_n I_b)$ , where  $B_z$  is the applied magnetic field normal to the horizontal surface of the SS,  $B_{c2}$  is the upper critical magnetic field of the SS at  $T=0$  K, and  $R_n$  is the normal resistance of the SS at  $T_c$ .  $R_n$ ,  $B_{c2}$ , and  $I_b$  are constants when these measurements are made. Therefore,  $V_{ib}$  is directly proportional to  $B_z$ . Figures 4(e) and 4(f) show the induced voltages  $V_{ib}$  as a function of the relative position of the magnets for positive and negative bias current, respectively. Notably, Fig. 4(e) is not the same as Fig. 4(b) because they show different components of the applied magnetic field. Also, the signs of  $V_{ib}$  are chosen to be consistent with the signs of  $V_{il}$ . When the direction of the electric field induced by the flow of flux inside the SS caused by the bias current is the same as that of the electric field induced inside the S–N loop due to Faraday’s law, the signs of both  $V_{ib}$  and  $V_{il}$  should be the same. For clockwise rotation, the center of the S–N loop will reach the magnet before the superconducting side of the loop does. Therefore, the induced voltage  $V_{ib}$

has a position delay with respect to the induced voltage  $V_{il}$ . Accordingly, for clockwise rotation with  $I_b = -100$  mA, Fig. 4(f) must be shifted to the right through a distance  $\Delta x/2$ , which equals approximately half of the width of the S–N loop, and then Fig. 4(c) is added to obtain the final induced voltage  $V_i$  as shown in Fig. 4(g), which is very similar to Fig. 3(c), in which the positive peak is much larger than the negative peak. For clockwise rotation with  $I_b = +100$  mA, the positive peak decreases much more than the negative peak. This result agrees with Fig. 3(b). For counterclockwise rotation of the magnets, Fig. 4(e) or Fig. 4(f) must be shifted to the left through a distance  $\Delta x/2$ , and then Fig. 4(d) is added when positive or negative bias currents are applied, respectively. Therefore, in these cases, the negative peak of  $V_i$  is affected much more strongly than the positive peak. These also agree with Fig. 3(e) and 3(f), and explain why  $V_{rms}$  depends strongly on both the direction of rotation of the PM and the bias current in this transition temperature region.

At temperature below the transition region, the critical current of the SS is much larger than the bias current  $I_b$ . That means that the vortex lines inside the SS cannot move or  $V_{ib}$  is negligibly small. Accordingly,  $V_{rms}$  becomes independent of  $I_b$ . However, some surprising findings must be explained.

1.  $V_{rms}$  decreases by approximately  $75 \mu\text{V}$  as the temperature  $T$  decreases from 93 to 87 K.

2.  $V_{rms}$  decreases as the temperature decreases.

3. Comparing the results for clockwise [Fig. 2(a)] and counterclockwise [Fig. 2(b)] rotation of the PM reveals that  $V_{rms}$  is always larger in the former case when the temperature is below 75 K.

The following explanation of the findings at temperature below the transition region is proposed. The magnetic field of a moving magnet is assumed not to be able to pass directly through the SS. Instead, some of the magnetic-field lines must first enter and then exit from all sides of the SS in accordance with Bean’s model.<sup>25,26</sup> The other magnetic-field lines have to bend in order to pass along the sides of the SS. Figure 5 shows the distribution of the vortices inside the SS as the magnets rotate clockwise at a particular temperature. The magnetic field  $\mathbf{B}_{af}$  in front of the SS must slightly exceed the stationary applied magnetic field  $\mathbf{B}_a$  to overcome the tension in the magnetic-field lines and cause them to curve around the SS. Similarly, the magnetic field  $\mathbf{B}_{ab}$  at the back of the SS must be slightly smaller than the stationary applied magnetic field  $\mathbf{B}_a$  to prevent the magnetic-field lines from curving excessively. Here,  $\mathbf{B}_{c1}$  represents the first critical field of the SS at that particular temperature. For YBCO superconductors,  $\mathbf{B}_{c1}$  is usually only a few tens of Gauss and its penetration depth is very small compared with the width of the SS. Therefore, its effect on our measurements is very weak and can be neglected. The total change of the magnetic flux ( $\Delta\Phi$ ) inside the SS should equal the shaded area in Fig. 5(b) multiplied by the distance between the two connected points on the SS for the induced voltage measurement. The upper boundary (V-shaped line) of the shaded area shows the magnetic-field distribution inside the SS as the external magnetic field increased to its maximum value. The lower boundary ( $\Lambda$ -shaped line) of the shaded area shows the magnetic-field distribution inside the SS as the external magnetic field decreased to its minimum value (nearly zero). The absolute

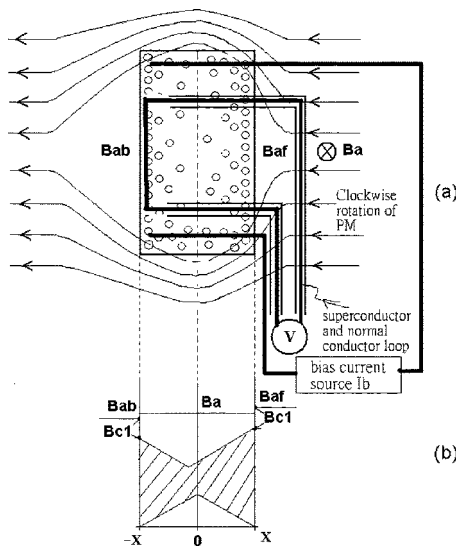


FIG. 5. (a) Schematic diagram of the distribution of vortices inside the SS and the superconductor-normal conductor loop, at the induced voltage  $V$  and at a particular temperature  $T$  in the low-temperature region. Here,  $\mathbf{B}_a$  is the applied magnetic field generated by the PM's,  $\mathbf{B}_{c1}$  is the first critical field of the SS at that temperature, and  $\mathbf{B}_{af}$  and  $\mathbf{B}_{ab}$  are the magnetic fields in the front and at the back, respectively, of the SS for the clockwise rotation of the PM's. (b) Average magnetic-field distributions inside the SS in accordance with Bean's model for increasing and decreasing the applied magnetic fields. The shaded area represents the change of the area occupied by the vortices as they enter and exit the SS.

values of the slope of both V-shaped and  $\Lambda$ -shaped lines should be proportional to the critical current density  $\mathbf{J}_c$  of the SS. As the temperature decreases, the critical current density  $\mathbf{J}_c$  increases. Therefore,  $\Delta\Phi$ , and thus the measured  $V_{\text{rms}}$ , should decrease as the temperature decreases. This answers point no. 2 in our findings. Figure 5(a) shows that the S-N loop consists of two parts. The left part is the area ( $A_s$ ) inside the SS. The right part is the area ( $A_n$ ) outside the SS. When the magnets rotate clockwise, as shown in the figure, the magnetic field  $\mathbf{B}_{af}$  in  $A_n$  is slightly larger than  $\mathbf{B}_a$ . However, if the magnets rotate counterclockwise, then the magnetic field in  $A_n$  becomes  $\mathbf{B}_{ab}$ , which is slightly smaller than  $\mathbf{B}_a$ .

This result explains our observation of  $V_{\text{rms}}$  at point no. 3. As to point no. 1 in our findings, we think this may be related to the manner in which the vortices move inside the SS. Whether some vortices can pass through the SS directly at a temperature around  $T_c$  (flux flow) or as shown in Fig. 5, some vortices simply enter from all sides of the SS first and then exit later at temperatures below the transition region.

#### IV. CONCLUSION

The root mean square of the voltage ( $V_{\text{rms}}$ ) induced inside a SS by the motion of a PM was measured. At a temperature around  $T_c$ ,  $V_{\text{rms}}$  is a sensitive function of both the bias current and the direction of motion of the magnets. The principle of superposition is applied to explain these phenomena. Two kinds of electric fields are induced inside the S-N loop. One is caused by the change of the magnetic flux inside the S-N loop. The other one is caused by the flow of the flux inside the SS under the influence of the bias current. Adding these two induced voltages inside the S-N loop according to the direction of the bias current and the direction of the rotation of the magnets yielded qualitative agreement with our experimental results. At temperatures below the transition region,  $V_{\text{rms}}$  first dropped to a certain value and then decreased as the temperature decreased. An explanation of how the magnetic field of a moving magnet passed through the SS was proposed, based on the assumption that some of the magnetic-field lines first entered and then exited from all sides of the SS in accordance with Bean's model. The other magnetic-field lines had to bend in order to pass along the sides of the SS. The change of the magnetic flux inside the S-N loop decreases as  $\mathbf{J}_c$  increases, so the induced voltage  $V_{\text{rms}}$  must decrease as the temperature decreases. This result also agrees qualitatively with the experimental results obtained at temperatures below the transition region.

#### ACKNOWLEDGMENT

This project was supported in part by the National Science Council of Taiwan under Grant No. NSC-92-2112-M-032-017.

<sup>1</sup>Y. B. Kim, C. F. Hempstead, and A. R. Strnad, *Phys. Rev.* **131**, 2486 (1963); Y. B. Kim, C. F. Hempstead, and A. R. Strnad, *ibid.* **139**, A1163 (1965).  
<sup>2</sup>A. K. Niessen and F. A. Staas, *Phys. Lett.* **15**, 26 (1965).  
<sup>3</sup>S. W. Tozer *et al.*, *Phys. Rev. Lett.* **59**, 1768 (1987).  
<sup>4</sup>S. J. Hagen *et al.*, *Phys. Rev. B* **43**, R6246 (1991).  
<sup>5</sup>T. R. Chien *et al.*, *Phys. Rev. Lett.* **66**, 3075 (1991).  
<sup>6</sup>R. Jin and H. R. Ott, *Phys. Rev. B* **57**, 13872 (1998).  
<sup>7</sup>Y. Yamamoto and K. Ogawa, *Physica C* **371**, 209 (2002).  
<sup>8</sup>R. H. Koch *et al.*, *Phys. Rev. Lett.* **63**, 1511 (1989).  
<sup>9</sup>E. Zeldov *et al.*, *Appl. Phys. Lett.* **56**, 680 (1990).  
<sup>10</sup>W. K. Kwok *et al.*, *Phys. Rev. Lett.* **73**, 2614 (1994).  
<sup>11</sup>G. D'Anna *et al.*, *Phys. Rev. Lett.* **75**, 3521 (1995).  
<sup>12</sup>M. C. Hellerqvist *et al.*, *Phys. Rev. Lett.* **76**, 4022 (1996).  
<sup>13</sup>D. Giller *et al.*, *Phys. Rev. Lett.* **79**, 2542 (1997).

<sup>14</sup>P. Berghuis *et al.*, *Phys. Rev. Lett.* **79**, 2332 (1997).  
<sup>15</sup>M. C. Cha and H. A. Fertig, *Phys. Rev. Lett.* **80**, 3851 (1998).  
<sup>16</sup>Y. Cao, Z. Jiao, and H. Ying, *Phys. Rev. B* **62**, 4163 (2000).  
<sup>17</sup>A. M. Petrean *et al.*, *Phys. Rev. Lett.* **84**, 5852 (2000).  
<sup>18</sup>Z. L. Xiao *et al.*, *Phys. Rev. Lett.* **85**, 3265 (2000).  
<sup>19</sup>B. J. Taylor *et al.*, *Phys. Rev. B* **68**, 054523 (2003).  
<sup>20</sup>S. Okuma and M. Kamada, *Phys. Rev. B* **70**, 014509 (2004).  
<sup>21</sup>I. G. Chen *et al.*, *J. Appl. Phys.* **81**, 4947 (1997).  
<sup>22</sup>B. D. Josephson, *Phys. Lett.* **16**, 242 (1965).  
<sup>23</sup>Y. B. Kim, C. F. Hempstead, and A. R. Strnad, *Phys. Rev.* **139**, A1163 (1965).  
<sup>24</sup>J. Bardeen and M. J. Stephen, *Phys. Rev. A* **140**, A1197 (1965).  
<sup>25</sup>C. P. Bean, *Phys. Rev. Lett.* **8**, 250 (1962); *Rev. Mod. Phys.* **36**, 31 (1964).  
<sup>26</sup>V. V. Moshchalkov *et al.*, *Physica C* **175**, 407 (1991).